Structural Requirements of the Fructan-Lipid Interaction

Ingrid J. Vereyken,* J. Albert van Kuik,† Toon H. Evers,* Pieter J. Rijken,* and Ben de Kruijff*
*Department Biochemistry of Membranes, Center for Biomembranes, Lipids, and Enzymology, Institute of Biomembranes, Utrecht University, The Netherlands; and †Department of Bio-Organic Chemistry, Section of Glycoscience and Biocatalysis, Bijvoet Center, Utrecht University, The Netherlands

ABSTRACT Fructans are a group of fructose-based oligo- and polysaccharides. They are proposed to be involved in membrane protection of plants during dehydration. In accordance with this hypothesis, they show an interaction with hydrated lipid model systems. However, the structural requirements for this interaction are not known both with respect to the fructans as to the lipids. To get insight into this matter, the interaction of several inulins and levan with lipids was investigated using a monomolecular lipid system or the MC 540 probe in a bilayer system. MD was used to get conformational information concerning the polysaccharides. It was found that levan-type fructan interacted comparably with model membranes composed of glyco- or phospholipids but showed a preference for lipids with a small headgroup. Furthermore, it was found that there was an inulin chain-length-dependent interaction with lipids. The results also suggested that inulin-type fructan had a more profound interaction with the membrane than levan-type fructan. MD simulations indicated that the favorable conformation for levan is a helix, whereas inulin tends to form random coil structures. This suggests that flexibility is an important determinant for the fructan-lipid interaction.

INTRODUCTION

Fructans are a group of fructose-based oligo- and polysaccharides. Based on the glycosidic linkage between the fructose units, they are divided in different classes; inulins containing exclusively $\beta(2 \rightarrow 1)$ linkages, levans containing mainly $\beta(2 \rightarrow 6)$ linkages, and graminans containing both linkage types (Fig. 1). Many different fungi, bacteria, and plants synthesize these molecules. In plants, fructans are accumulated in the vacuole, but they are also found in the phoem (Wang and Nobel, 1998). Fructans serve as carbohydrate storage. In addition, fructans also have been implicated in playing a role in cold and drought tolerance (Hendry, 1993; Pontis, 1989; Vijn and Smeekens, 1999; Konstantinova et al., 2002). The natural distribution of these plants coincides with regions that have a temperate to subtropical climate with seasonal or more sporadic rainfall (Hendry, 1993). However, fructan-accumulating plants also grow in deserts, e.g., *Agave* spp. Furthermore, fructan accumulation is induced during drought in species which are capable of synthesizing these compounds (Roover et al., 2000). In addition, a levan-type fructan-accumulating transgenic tobacco plant shows enhanced drought tolerance compared to the wild-type control plant (Pilon-Smits et al., 1995).

Membranes are the primary targets of both freezing and desiccation injury in cells; therefore, it was hypothesized that fructans have a direct interaction with membranes, thereby stabilizing them under dry conditions (Demel et al., 1998).

Model membrane studies have revealed that fructans do have an interaction with lipids (Vereyken et al., 2001; Demel et al., 1998). Under hydrated conditions levan interacts with different phospholipids both in mono- and bilayer systems. They increase the temperature of the L_α-H_{II} transition of 1,2-dielaidoyl-*sn*-glycero-3-phosphoethanolamine (DEPE) by 4°C, indicating that they stabilize the L_α phase (Vereyken et al., 2001). It was reported that levan interacts much stronger with membrane lipids than dextrans (Vereyken et al., 2001), suggesting specificity for the polysaccharide. Inulin also inserts into a phospholipid monolayer (Demel et al., 1998). Thus it appears that it is a general property of fructan to interact with lipids.

Under dry conditions inulin lowered the phase transition temperature of egg phosphatidylcholine (PC) of the gel to liquid crystalline phase by ~20°C as measured using FT-IR (Hincha et al., 2000), thereby stabilizing the L_α phase. Moreover, inulins were able to reduce the amount of carboxyfluorescein leakage from liposomes consisting of PC, which were rehydrated after drying (Hincha et al., 2000; Hincha et al., 2002). These findings support the view that fructans can have a membrane-protecting role in plants during drought.

The structural requirements of the fructan-lipid interaction are not very well known. Our previous findings suggest that levans have a preference for PE (Vereyken et al., 2001). This could be explained either by a specific interaction between the two compounds or a more general preference of levans for lipids with a smaller headgroup. In this study we want to discriminate between those two options. In addition, it is also investigated whether fructans can interact with

Submitted October 17, 2002, and accepted for publication January 21, 2003.

Address reprint requests to Ingrid J. Vereyken, Dept. Biochemistry of Membranes, Utrecht University, Padualaan 8, 3584 CH Utrecht, The Netherlands. Fax: +31-30-2533969; E-mail: i.j.vereyken@chem.uu.nl.

List of abbreviations: MC 540, merocyanine 540; MD, molecular dynamics; PE, phosphatidylethanolamine; PC, phosphatidylcholine; DPPC, 1,2-dipalmitoyl-*sn*-glycero-3-phosphocholine; DMPC, 1,2-dimyristoyl-*sn*-glycero-3-phosphocholine; DOPC, 1,2-dioleoyl-*sn*-glycero-3-phosphocholine; $DOPENMe_2$, 1,2-dioleoyl-*sn*-glycero-3-phosphoethanolamine-*N, N*-dimethyl; DOPE, 1,2-dioleoyl-*sn*-glycero-3-phosphoethanolamine; MGDG, monogalactosyldiglyceride; DGDG, digalactosyldiglyceride; AUS, adaptive umbrella sampling; PMF, potential of mean force; LUVETs, large unilamellar vesicles prepared by extrusion technique.

0006-3495/03/05/3147/08 $2.00

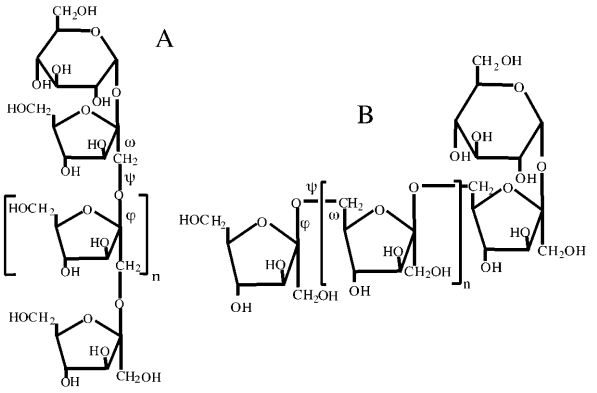

FIGURE 1 The structure of inulin (*A*) and levan (*B*) type fructan. The Greek symbols refer to the angles that are used in the MD simulation (see Results).

membrane glycolipids, monogalactosyldiglyceride (MGDG) and digalactosyldiglyceride (DGDG), which are abundantly and uniquely present in plants. Next to lipid specificity, the required interaction properties for the carbohydrates are not well understood either. Little is known about the inulin-lipid interaction or about the importance of fructan linkage type and size.

To get insight into these questions, the interaction of different fructans with a mono- and bilayer lipid system was analyzed under hydrated conditions. To get a better understanding of the fructan-lipid interaction, the influence of linkage type on the three-dimensional structure of the fructans was investigated by molecular dynamics.

Levan interacted more favorably with the lipids with a smaller headgroup. The fructan-lipid interaction was found to be dependent on the type and length of the fructan and appeared to be determined by the conformational properties of the polysaccharide.

MATERIALS AND METHODS

Materials

1,2-dipalmitoyl-*sn*-glycero-3-phosphocholine (DPPC); 1,2-dimyristoyl-*sn*-glycero-3-phosphocholine (DMPC); 1,2-dioleoyl-*sn*-glycero-3-phosphocholine (DOPC); 1,2-dioleoyl-*sn*-glycero-3-phosphoethanolamine-*N*-methyl (DOPENMe); 1,2-dioleoyl-*sn*-glycero-3-phosphoethanolamine-*N,N*-dimethyl (DOPENMe$_2$); and 1,2-dioleoyl-*sn*-glycero-3-phosphoethanolamine (DOPE) were obtained from Avanti Polar Lipids (Alabaster, AL). MGDG and DGDG isolated from corn germ were purchased from Unipure. Merocyanine 540 (MC 540) and dextran were obtained from Sigma (Zwÿndrecht, the Netherlands).

The chain length of the different fructans used in this study is given as the average degree of polymerization (DP). Levan (DP 125, 25 kDa) was isolated from *B. subtilis* as described by Vereyken et al. (Vereyken et al., 2001). Inulin DP 10 (Frutavit IQ) and Inulin DP 21 (Raftiline HP) were kind gifts of Sensus (Roosendaal) and ATO-DLO (Wageningen), respectively. Inulin DP 26 (dahlia inulin) was obtained from Sigma.

Vesicle preparation

LUVETs were prepared by extrusion according to Hope et al. (Hope et al., 1985). Lipids dissolved in chloroform were dried using rotational evaporation. After storage of the lipid film for at least 2 h under high vacuum, the lipids were dispersed in 10 mM Tris/HCl pH 7.5 above their gel to liquid-crystalline phase transition temperature and under mechanical agitation. The sample was freeze/thawed 10 times in a CO_2/ethanol bath and subsequently extruded 10 times through two stacked 400 nm membrane filters.

The lipid-phosphate concentration in the resulting solutions was determined according to Rouser et al. (Rouser et al., 1970).

Monolayer experiments

Measurements at constant surface area

The surface tension was measured using the Wilhelmy plate method (Demel, 1994). Experiments were performed in a 2.0 ml dish at room temperature (±21°C). MiliQ-water was used as subphase, on which a lipid layer was spread until a surface pressure between 20 and 35 mN/m was reached. Polysaccharides were added to the subphase through a small injection hole while the subphase was continuously stirred. Within ~30 min, the pressure increase stabilized. The change in surface pressure at that time point was taken as a measure for the interaction of the polysaccharides with the lipids. In the absence of a lipid film the polysaccharides themselves showed a surface pressure increase >0.6 mN/m (Vereyken et al., 2001).

Pressure-area measurements

Pressure-area curves were measured after spreading of 5 nmol lipid on a surface of 65 cm^2. As subphase either water or an 8 mg/ml fructan solution was used. After 10 min equilibration, the lipid layer was compressed until close to the collapse pressure with a rate of 15 cm^2/min, and subsequently the lipid layer was expanded at the same rate. Expansion and compression were repeated several times and found to give reproducible results.

MC 540 partitioning

The surface properties of a vesicle can be accessed by the probe molecule MC 540 (Stillwell et al., 1993). The partitioning of the probe between hydrophobic and hydrophilic environment depends on the packing of the headgroup region. The ratio between the absorption at 530 nm and 570 nm is a measure for this partitioning (Bakaltcheva et al., 1994). LUVETs were made as described (see Vesicle preparation). In the sample 0.5 mM lipid was incubated at 30°C with the appropriate amount of carbohydrates in a final volume of 1 ml. After 30 min, 2 μl of an ethanol/water (1:2 v/v) solution of the dye was added resulting in a final dye concentration of 6.6 μM. The mixture was incubated for another five min. Next, the mixture was transferred into a 1 ml cuvet and the absorption of MC 540 was measured in a Perkin Elmer Lambda 18 UV/VIS Spectrometer.

Molecular dynamics

To analyze the population distribution for the glycosidic dihedral angles, PMF calculations were performed with the GROMOS improved forcefield for carbohydrates (Spieser et al., 1999) using the method of AUS (Hooft et al., 1992). All simulations were divided into 72 classes, each having a width of 5°. The derivative of the PMF was evaluated as a 12-term Fourier series. Each system was simulated for at least 10 ns, and the final PMF for each system was used to obtain the rotamer population distribution of the sampled dihedral angle.

MD simulations in water were performed using the GROMACS program (Lindahl et al., 2001) with the GROMOS forcefield (Spieser et al., 1999), and the SPC/E water model (Berendsen et al., 1987). Periodic boundary conditions were applied by placing all molecules in a computational truncated octahedral periodic box. All bond lengths were kept fixed using the SHAKE procedure (Ryckaert et al., 1977). Simulations were performed with loose coupling to a pressure bath at 1 atm and a temperature bath at 300 K

(Berendsen et al., 1984) with time constants of 0.5 and 0.1 ps, respectively. For the simulation, a cutoff radius of 1.0 nm, a time step of 2 fs, and a total simulation time of 10 ns was used. A hydrogen bond is considered to be present for donor H and acceptor O atoms with a H··O distance of <2.5 Å and an O-H··O bond angle >120°.

RESULTS

Lipid specificity

Previous studies showed that levans caused a larger surface pressure increase using PE than using PC monolayer systems, suggesting a preferential interaction with PE (Vereyken et al., 2001). This could either be explained by the specific nature of this headgroup or be due to a more general phenomenon, namely that levan has a preference for smaller headgroups. This is why we chose to measure the surface pressure increase in a monolayer consisting of DOPE or the methylated forms of this lipid, DOPENME having one methyl group, $DOPENME_2$ having two methyl groups, and DOPC having three methyl groups attached. The injection of 8 mg/ml levan underneath the monolayer caused a surface pressure increase in all cases (Fig. 2), indicating that levan is capable of interacting with all of these different lipids. However, it is also clear from Fig. 2 that levan caused the largest pressure increase in the DOPE monolayer, whereas no significant differences in pressure increase were observed for the methylated forms including DOPC.

To investigate the question of the headgroup size versus specific interaction further, monolayer experiments were performed using MGDG and DGDG. These plant specific glycolipids contain either one (MGDG) or two (DGDG) galactosyl residues attached to the glycerol backbone. Both lipids formed stable monolayers. Injection of levan caused an increase in surface pressure (Fig. 3), demonstrating the interaction between levan and glycolipids. The surface pressure increase for MGDG is higher than for DGDG, suggesting a preference of the levan for the lipid with the smaller headgroup.

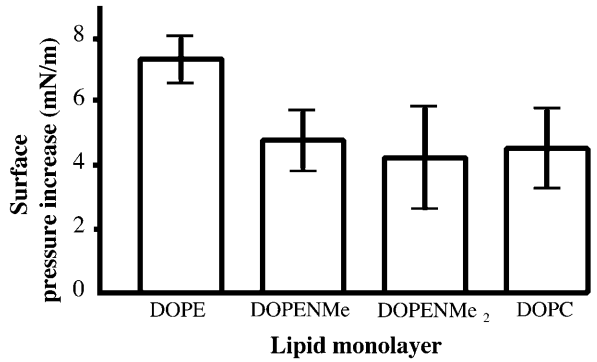

FIGURE 2 The effect of headgroup size on the interaction of fructan with phospholipids making use of PE and the methylated forms of PE. Surface pressure increase induced by 8 mg/ml levan at an initial surface pressure of 20 mN/m.

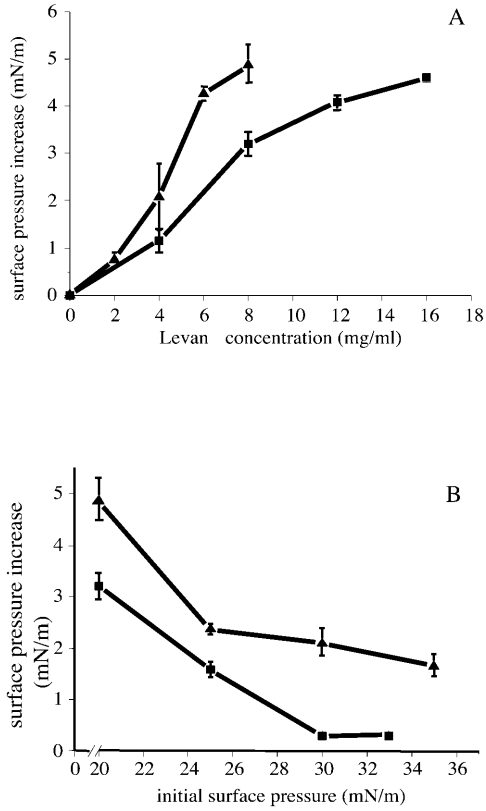

FIGURE 3 The effect of levan on the plant lipids MGDG and DGDG. (*A*) Surface pressure increase induced by different concentrations of levan on a (▲) MGDG monolayer or a (■) DGDG monolayer spread at 20 mN/m. (*B*) Surface pressure increase induced by 8 mg/ml levan as a function of the initial surface pressure of a (▲) MGDG monolayer or a (■) DGDG monolayer.

In Fig. 3 *B* the relation between the initial surface pressure (lipid packing density) and the surface pressure increase is shown. Increasing the initial surface pressure resulted in a gradual decrease in insertion of levan for both MGDG and DGDG. Interestingly, at a surface pressure of 30 mN/m, which is thought to be equivalent to a packing density of lipids in natural membranes (Seelig, 1987), levan still showed a substantial interaction with the MGDG monolayer but hardly showed an effect on DGDG.

Carbohydrate specificity

To get insight into the carbohydrate specificity of the fructan-lipid interaction, we also studied the interaction of inulin-type fructans with membrane lipids. In addition, the influence of the inulin size was investigated by using inulins with a different degree of polymerization. DPPC was chosen as the lipid model system for monolayer experiments because it shows both a liquid-expanded and a liquid-condensed state. Furthermore, the obtained results can be directly compared to the data of levan-type fructan obtained earlier (Vereyken et al., 2001). Pure DPPC showed a phase transition from liquid-expanded to liquid-condensed state at 5 mN/m

(Fig. 4 *A*) as reported in the literature (Demel et al., 1998). Upon the addition of the largest inulin-type fructan, inulin DP 26, the curve was substantially shifted to larger areas both in the liquid-expanded and the liquid-condensed state. In addition, the phase transition nearly vanished. This demonstrates the penetration of inulin into the monolayer under both lipid packing conditions. Interestingly, decreasing the length of the inulin caused a reduction in penetration. However, even inulin DP 10 showed a substantial expansion of the monolayer. Similar results were obtained for DMPC monolayers, which are in the liquid-expanded state at room temperature (Fig. 4 *B*). These results suggest a strong dependency of the lipid interaction on the length of the fructan molecule.

To investigate the inulin-lipid interaction in a bilayer model system, the effect of carbohydrates on the partitioning of the amphipathic dye MC 540 between DMPC LUVETs and the water phase was analyzed at 30°C. Partitioning is reflected by the absorbance ratio A570/A530; upon entering a hydrophobic environment the absorbance at 570 nm increases, whereas the absorption maximum at 530 nm is slightly reduced (Bakaltcheva et al., 1994; Vereyken et al., 2001). Fig. 5 shows that the largest inulin gave the largest reduction in the A570/A530 ratio. This indicates that inulin DP 26 interacts with the bilayer and thereby reduces the ability of MC 540 to partition into the lipid layer. The smaller inulins reduced the A570/A530 ratio less, which is in accordance with the monolayer data.

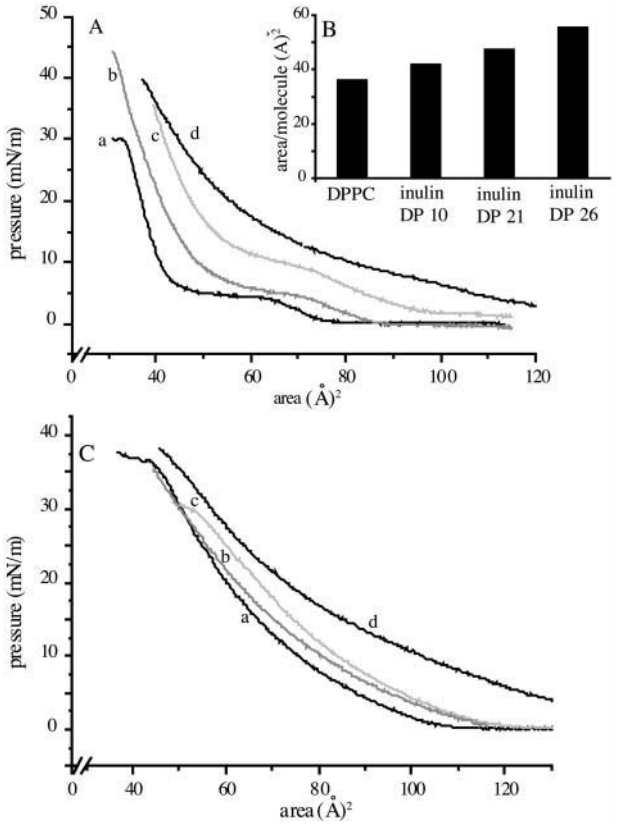

FIGURE 4 The effect of the length of the inulin chain on the surface pressure of PC lipids. In all experiments 8 mg/ml inulin was used. (*A*) Pressure-area curve of DPPC monolayer in the absence (*line a*) and the presence of inulin DP 10 (*b*) inulin DP 21 (*c*) and inulin DP 26 (*d*). (*B*) The difference in monolayer expansion seen in the pressure area curve of DPPC in the absence and presence of carbohydrates at 20 mN/m. (*C*) Pressure-area curve of a DMPC monolayer in the absence (*line a*) and the presence of inulin DP 10 (*b*) inulin DP 21 (*c*) and inulin DP 26 (*d*).

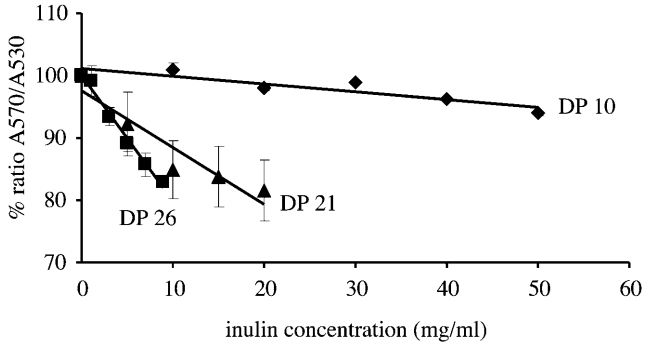

FIGURE 5 The effect of the differences in chain length of inulin on the partitioning of MC 540 between water and DMPC vesicles. A total of 0.5 mM of DMPC LUVETs was mixed with the indicated amount of polysaccharide and incubated for 30 min at 30°C. MC 540 was added, and after 5 min the A570/A530 ratio was measured. In the absence of polysaccharide the ratio was set to 100%. (♦) Inulin DP 10, (▲) inulin DP 21, and (●) inulin DP 26.

We previously observed (Vereyken et al., 2001) that MC 540 can directly bind to levan indicating the presence of hydrophobic sites in this polysaccharide. Therefore, we analyzed the interaction of inulin-type fructan with MC 540 in the absence of vesicles. In Fig. 6 it is shown that the largest inulin gave the largest increase in the A570/A530 ratio. Based on Bakaltcheva et al. (Bakaltcheva et al., 1994) this can be interpreted as an increase in the hydrophobicity of the environment of the dye, which suggests that the inulin DP 26 also contains hydrophobic sites. In addition, the shorter inulins increased the ratio to a lesser extent, suggesting that

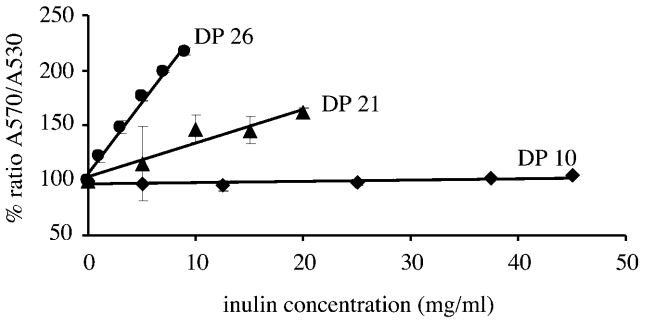

FIGURE 6 The effect of the differences in chain length of inulin on the A570/ A530 ratio of MC540. The indicated amount of polysaccharide was incubated for 15 min at 30°C. MC540 was added and after 5 min the A570/ A530 ratio was measured. In the absence of polysaccharide the ratio was set to 100%. (♦) Inulin DP 10, (▲) inulin DP 21, and (●) inulin DP 26.

they contain fewer hydrophobic sites. It should be noted that the spectral changes observed for the fructan-dye interaction are much smaller in absolute value than the changes observed in the presence of lipid vesicles (data not shown). The data in Fig. 5 are not corrected for this small effect but would probably be somewhat larger than measured, since counteracting spectral changes are observed compared to the fructan-dye interaction. In conclusion, these results suggest that longer inulin chains are more hydrophobic than shorter inulin chains, which provides an explanation for the increased lipid interaction of the longer inulins.

Molecular dynamics

Molecular understanding of the interaction of inulin and levan with lipids requires knowledge of the spatial structure of the carbohydrates. Some work has been done on the conformations in crystal structures of smaller fructan molecules and by molecular mechanics calculations in vacuo (Calub et al., 1990; Ferretti et al., 1983; French et al., 1997; Jeffrey and Park, 1972; Liu and Waterhouse, 1992; Waterhouse et al., 1991). However, little is known of the conformation of larger structures in solution, and therefore MD simulations of model compounds in the presence of water molecules were performed. Conformational differences between polysaccharides are usually located in the glycosidic linkages of the backbone. The linear fructans levan and inulin have a backbone that consists of three rotatable bonds. In levan, the furanoses are (2 → 6) linked with linkages φ(O5′-C2′-O6-C6), ψ(C2′-O6-C6-C5), and ω(O6-C6-C5-C4) whereas for the (2 → 1) linked inulin these are φ(O5′-C2′-O1-C1), ψ(C2′-O1-C1-C2) and ω(O1-C1-C2-C3). The ω dihedral angle is usually the most flexible. The population distribution of these angles in water was explored by AUS of the PMF. The minimal energy structures derived from crystal structures and molecular mechanics calculation in vacuo were used as starting conditions and are described in the appendix. The dihedral angles φ and ψ are found essentially at one position (−70° and 170°, respectively) as shown in the appendix. Investigating the dihedral angle ω, levanbiose showed a strong preference for one conformation for which ω is 50°, whereas inulobiose accommodates two major and one minor conformations, namely with ω at 50°, 165°, and −70° (44:44:12, respectively) as depicted in Fig. 7.

The dihedral angles resulting from this calculation were used to perform MD simulations in water on structures containing 10 fructofuranose residues with each end terminated by a α-D-Glc*p*, β-D-Fru*f*-(2 → [6)-β-D-Fru*f*-(2]$_9$ → 1)-α-D-Glc*p*, denoted LEV10, and β-D-Fru*f*-(2 → [1)-β-D-Fru*f*-(2]$_9$ → 1)-α-D-Glc*p*, denoted INU10. The starting structure was built in agreement with the most favorable conformation, which resulted in a helix-like structure in the case of LEV10. Within 10 ps the structure adopted a right-handed helix with 5 units per two turns of the helix and did not lose this conformation during the remainder of the simulation (Fig. 8 *A*). This conformation was stabilized by hydrogen bonds from the donor hydroxyl at C3 of residue *i* to the acceptor O5 of residue *i*-2 (O3(*i*)-H3(*i*)···O5(*i*-2), Table 1). Note that the first and the last hydrogen bond show a lower percentage, suggesting more flexibility at both ends. Considering that a few percent of ω is expected to be at 180° (50°:175° = 93:7), which will interrupt the helix, levan with DP > 100 is anticipated to consist of helical parts with an average length of ~14 units. These estimations are based only on the PMF calculated for the disaccharide. The hydrogen bond interactions can make the helix more favorable.

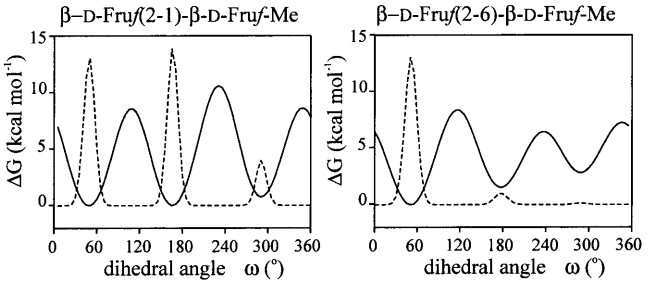

FIGURE 7 Potential of mean force (*solid line*) and population distribution (*dashed line*) of the ω dihedral angle of levanbiose (*left panel*) and inulobiose (*right panel*). Population distribution of the ω dihedral angle of levanbiose 50°:175° = 93:7, and of inulobiose 50°:165°:−70° = 44:44:12.

The population distribution profile of the ω dihedral angle of INU10 indicated many favorable conformations. Two MD simulations were performed, one with ω initially at 60° and one with ω at 180° for all Fru-(2 → 1)-Fru linkages. During

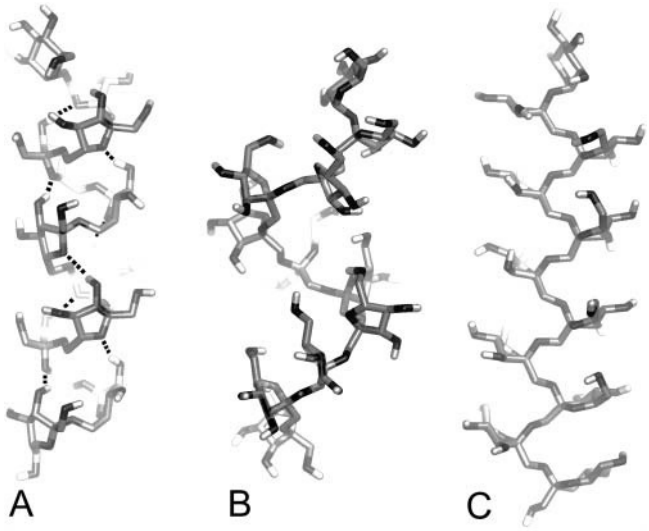

FIGURE 8 Snapshots of typical conformations from the MD simulations. The preferred conformation of LEV10 (*A*), a right-handed helix with five units per two turns. Hydrogen bonds are indicated by dashed lines. Two favored conformations of INU10, a right-handed sixfold helical structure (*B*), with all ω dihedral angles at 60°, and a zigzag structure (*C*), with all ω dihedral angles at 180°.

TABLE 1 Occurrence of O3(*i*)-H3(*i*)···O5(*i*-2) hydrogen bond during a 10 ns MD simulation of LEV10

Residue number *i*	Percentage of hydrogen bonds during simulation
10	39
9	79
8	81
7	79
6	80
5	82
4	81
3	38

the first simulation, with ω at 60°, many conformations including right-handed helix-like structures with 4, 5, or 6 units per turn were observed (Fig. 8 *B*). From these observations, it is concluded that inulin is rather flexible, in particular at both ends. This could be due to the lack of stabilizing hydrogen bonds, and also because 10 fructose residues are probably not enough to form a stable helix, if indeed any stable helix can be formed. The second MD run, with ω at 180°, showed a zigzag conformation that did not change during the 10 ns simulation (Fig. 8 *C*). No typical hydrogen bonds were observed in either MD simulation, nor did any transitions occur of the glycosidic linkages. Considering the distribution profile of the ω dihedral angle and the observed flexibility in the first simulation, many more conformations seemed to be possible. Therefore it is very likely that inulin is a random coil in solution.

DISCUSSION

The aim of this study was to get insight into the structural requirements of both lipids and fructans for the lipid-fructan interaction. It was found that levan penetrated most extensively in a monolayer composed of DOPE compared to its methylated forms. Comparing the different glycolipids MGDG and DGDG, the largest pressure increase was observed for MGDG. Furthermore, a chain length dependency was found for interaction of inulin with lipids. MD simulations, in solution, suggested that the favorable conformation for levan is a helix, whereas inulin tends to form random coil structures. All these data gave more insight into the requirements of the fructan-lipid interaction.

Lipid specificity

To investigate whether headgroup size is important for the fructan-lipid interaction, DOPE and the methylated forms of DOPE (including DOPC) were investigated. Levan displayed the largest insertion into a DOPE monolayer and showed a similar insertion into all the other monolayers consisting of the methylated forms of DOPE. Chemically these headgroups are similar, since they are all zwitterionic, and PE and its mono- and dimethylated analogs have hydrogen-bonding possibilities. The most striking difference between these lipids is their L_α-H_{II} phase transition temperature, which is by far the lowest for DOPE (Gagne et al., 1985). In terms of the shape-structure concept of lipid polymorphism (Cullis and de Kruijff, 1979), this means that DOPE has the smallest headgroup, which suggests that the small size of the PE headgroup promotes the levan-lipid interaction.

Glycolipids were investigated to test whether the headgroup size dependency is a general property of the levan-lipid interaction. MGDG has a smaller headgroup than DGDG and consequently has the lowest L_α-H_{II} phase transition temperature (Shipley et al., 1973). In analogy to PE, levan penetrated most strongly into the MGDG monolayer. Therefore, it can be concluded that the fructan-lipid interaction shows a preference for a small headgroup size. Several explanations can be proposed for this observation. We favor the explanation based on the preferential insertion of peripheral proteins in mono- and bilayers composed of lipids with a small headgroup as provided by van den Brink-van der Laan et al. (2001). In that study it was proposed that smaller headgroups result in less densely packed surfaces, leading to the exposure of more hydrophobic surface at the interface, thereby creating the so-called hydrophobic interfacial insertion sites. These sites could facilitate the levan-lipid interaction.

In addition, other conclusions can be drawn from the observed interaction between levan and the glycolipids. Neither MGDG nor DGDG contains a phosphate group, and levan interacts with both lipids. Thus it can be concluded that the phosphate group is not essential for the fructan-lipid interaction. Furthermore, levan induced a similar pressure increase using comparable concentrations in a monolayer consisting of glycolipids or in a monolayer composed of phospholipids. This suggests that specific interactions between the levan and the galactose headgroup do not play a major role in the interaction.

Carbohydrate specificity

Inulins inserted into the lipid monolayer and showed an interaction with the lipid bilayer, as did levan (Demel et al., 1998; Vereyken et al., 2001). Therefore, it can be concluded that fructans have an interaction with lipids. Dextran, a glucan, hardly showed an interaction with the lipid monolayer (Vereyken et al., 2001), indicating that it is not an intrinsic property of polysaccharides in general. In addition, for the dextran-lipid interaction there was no chain length dependency observed for DP 10 to approximately DP 200 (unpublished results). The most striking difference between the polysaccharides is that dextrans are branched polysaccharides with relatively large and rigid pyranose rings (Barrows et al., 1995), whereas levan and inulin are mainly linear fructose polymers, composed of less bulky and more flexible furanose rings (French and Waterhouse, 1993). This flexibility could be crucial for a substantial membrane interaction.

There was a distinct inulin chain length dependency in the inulin-lipid interaction. Both in the monolayer and the MC 540 experiments it was observed that the extent of lipid interaction followed the same order: inulin DP 26 > inulin DP 21 > inulin DP 10. This is in accordance with data obtained for smaller inulins under dehydrated conditions (Hincha et al., 2002). This suggests that data found under hydrated conditions concerning the fructan-lipid interaction could be extrapolated to conditions with less water. In addition, in the MC 540 experiment without vesicles, it was observed that the interaction with the dye was stronger with longer inulin chains, indicating that they are more hydrophobic. This could be an explanation for the size dependency of the lipid-inulin interaction.

Although inulin and levan both showed an interaction with lipids, differences can be observed. Levan-type fructan had a DP of 125. Yet its lipid interaction corresponds to an inulin, which has a DP of ~15. This suggests that levan has a less profound lipid interaction than inulin.

The results obtained in the MD simulations offer insight into the specificity of the fructan-lipid interaction. The MD simulations showed that inulin can adopt many different conformations. Larger molecules can adopt more preferred conformations for membrane binding within one molecule than smaller ones, resulting in more interaction points per inulin, which strengthens the inulin-lipid interaction. The MC 540 experiments indeed show that a larger molecule has a stronger interaction with the probe, which could either reflect the overall hydrophobicity of the molecule or could point to more potential membrane binding sites within one molecule.

Concerning the difference between inulin and levan, it is conceivable that the large flexibility of inulin makes it easier to adopt the preferred conformation to bind to the membrane, whereas levan is more inclined to maintain the favorable helix conformation. Another difference between levan and inulin is the position of the furanose rings. In levan the furanose rings are part of the backbone, whereas inulin can be considered a polyethylene oxide backbone with furanose rings attached to it. Possibly, this makes it easier for the rings to interact with the membrane.

In conclusion, the data suggest that the flexibility and the hydrophobicity of the polysaccharide are important factors in determining the extent of polysaccharide-lipid interaction.

TABLE 2 Dihedral angles of the glycosidic linkages of fructans

	Levanbiose		6-kestose	Inulobiose		1-kestose	
φ	−70	−77*	−56†	−70	−69‡	−41§	−60¶
ψ	165	166*	146†	170	169‡	−170§	−162¶
ω	50	56*	−177†	50/165	178‡	−59§	−60¶

*Liu and Waterhouse (1992)
†Ferretti et al. (1983)
‡Calub et al. (1990)
§Jeffrey and Park (1972)
¶Waterhouse et al. (1991)

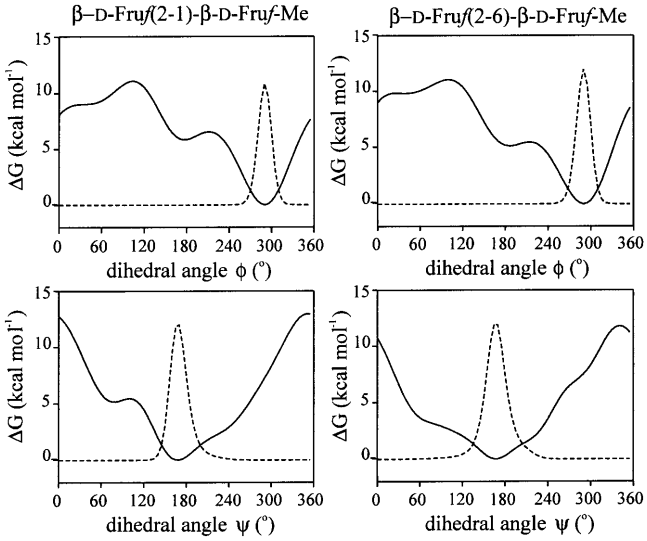

FIGURE A1 Potential of mean force (*solid line*) and population distribution (*dashed line*) of the ψ and φ dihedral angle of levanbiose (*right panel*) and inulobiose (*left panel*).

APPENDIX: MOLECULAR DYNAMICS

Crystallographic data

Crystallographic data of 6-kestose, and molecular mechanics analysis of levanbiose, detected a preference for φ near −60° and ψ near 180° (Table 2). From crystallographic data of 1-kestose and molecular mechanics analysis of inulobiose, φ and ψ were located in the neighborhood of −60° and 180°, respectively. The ω dihedral angle is usually the most flexible and gives different values for crystallographic structures and structures that were minimized by molecular mechanics calculations.

Adaptive umbrella sampling

To estimate the population distribution of the glycosidic linkages in water, the method of AUS of the PMF was used (Hooft et al., 1992) with the methyl-glycosides of levanbiose and inulobiose, the disaccharides β-D-Fruf-(2 → 6)-β-D-Fruf-Me and β-D-Fruf-(2 → 1)-β-D-Fruf-Me, respectively. AUS simulations were performed by applying an umbrella potential to one dihedral angle per simulation. From the final PMF the population distributions were calculated. The differences in conformational behavior between both disaccharides are located in the population distributions of the ω dihedral angles (Fig. 7), where φ and ψ behave similar for both carbohydrates (Fig. A1). Dihedral angles of the glycosidic linkages, obtained from the AUS simulations, are given in Table 2.

The starting conformation of LEV10 was based on these data. All Fru-(2 → 6)-Fru glycosidic linkages were set at φ:ψ:ω = −60°:180°:60°. The Fru-(2 → 1)-Glc in INU10 linkages were set to φ (O5(G)-C1(G)-O1(G)-C2(F)) at 80° and ψ (C1(G)-O1(G)-C2(F)-C3(F)) at −170° in agreement with the crystallographic data of 6-kestose (Ferretti et al., 1983).

This research was supported by an Earth and Live Sciences (ALW) and chemical sciences (CW) grant with financial aid from the Dutch Organization for Scientific Research (NWO). Additional support came from CW/STW project 349-4608 with financial aid from NWO.

REFERENCES

Bakaltcheva, I., W. P. Williams, J. M. Schmitt, and D. K. Hincha. 1994. The solute permeability of thylakoid membranes is reduced by low concentrations of trehalose as a co-solute. *Biochim. Biophys. Acta.* 1189:38–44.

Barrows, S. E., F. J. Dulles, C. J. Cramer, and A. D. French. 1995. Truhlar. Relative stability of alternative chair forms and hydroxymethyl conformations of β-D-glucopyranose. *Carbohydr. Res.* 276:219–251.

Berendsen, H. J. C., J. R. Grigera, and T. P. Straatsma. 1987. The missing term in effective pair potentials. *J. Phys. Chem.* 91:6269–6271.

Berendsen, H. J. C., J. P. M. Postma, W. F. van Gunsteren, A. DiNiola, and J. R. Haak. 1984. Molecular dynamics with coupling to an external bath. *J. Chem. Phys.* 81:3684–3690.

Calub, T. M., A. L. Waterhouse, and A. D. French. 1990. Conformational analysis of inulobiose by molecular mechanics. *Carbohydr. Res.* 207:221–235.

Cullis, P. R., and B. de Kruijff. 1979. Lipid polymorphism and the functional roles of lipids in biological membranes. *Biochim. Biophys. Acta.* 559:399–420.

Demel, R. A. 1994. Monomolecular layers in the study of biomembranes. *In* Physicochemical Methods in the Study of Biomembranes. H. J. Hilderson and G. B. Ralston, editors. Plenum Press, New York. 83–120.

Demel, R. A., E. Dorrepaal, M. J. M. Ebskamp, J. C. M. Smeekens, and B. de Kruijff. 1998. Fructans interact strongly with model membranes. *Biochim. Biophys. Acta.* 1375:36–42.

De Roover, J., K. Vandenbranden, A. V. Laere, and W. Van den Ende. 2000. Drought induces fructan synthesis and 1-SST (sucrose:sucrose fructosyltransferase) in roots and leaves of chicory seedlings (*Cichorium intybus L.*). *Planta.* 210:808–814.

Ferretti, V., V. Bertolasi, and G. Gilli. 1983. Structure of 6-kestose monohydrate, *C18H31O16.H2O. *Acta Crystallogr.* C40:531–535.

French, A. D., M. K. Dowd, and P. J. Reilly. 1997. MM3 modeling of fructose ring shapes and hydrogen bonding. *J. Mol. Struct.* 395–396:271–287.

French, A. D., and A. L. Waterhouse. 1993. Chemical structure and characteristics. *In* Science and Technology of Fructans. M. Suzuki and N. J. Chatterton, editors. CRC Press, Boca Raton. 41–81 p.

Gagne, J., L. Stamatatos, T. Diacovo, S. Wen Hui, P. L. Yeagle, and J. R. Silvius. 1985. Physical properties and surface interactions of bilayer membranes containing N-methylated phosphatidylethanolamines. *Biochemistry.* 24:4400–4408.

Hendry, G. A. F. 1993. Evolutionary origins and natural functions of fructans - a climatological, biogeographic and mechanistic appraisal. *New Phytol.* 123:3–14.

Hincha, D. K., E. M. Hellwege, A. G. Heyer, and J. H. Crowe. 2000. Plant fructans stabilize phosphatidylcholine liposomes during freeze-drying. *Eur. J. Biochem.* 267:535–540.

Hincha, D. K., E. Zuther, E. M. Hellwege, and A. G. Heyer. 2002. Specific effects of fructo- and gluco-oligosaccharides in the preservation of liposomes during drying. *Glycobiology.* 12:103–110.

Hooft, R. W. W., B. P. van Eijck, and J. Kroon. 1992. An adaptive umbrella sampling procedure in conformational analysis using molecular dynamics and its application to glycol. *J. Chem. Phys.* 97:6690–6694.

Hope, M. J., M. B. Bally, G. Webb, and P. R. Cullis. 1985. Production of unilamellar vesicles by rapid extrusion procedure characterisation of size distribution trapped volume and ability to maintain a membrane potential. *Biochim. Biophys. Acta.* 812:55–65.

Jeffrey, G. A., and Y. J. Park. 1972. The crystal and molecular structure of 1-kestose. *Acta Crystallogr.* B28:257–267.

Konstantinova, T., D. Parvanova, A. Atanassov, and D. Djilianov. 2002. Freezing tolerant tobacco, transformed to accumulate osmoprotectants. *Plant Sci.* 163:157–164.

Lindahl, E., B. Hess, and D. van der Spoel. 2001. GROMACS 3.0: a package for molecular simulation and trajectory analysis. *J. Mol. Model.* 7:306–317.

Liu, J., and A. L. Waterhouse. 1992. Conformational analysis of levanbiose by molecular mechanics. *Carbohydr. Res.* 232:1–15.

Pilon-Smits, E. A. H., M. J. M. Ebskamp, M. J. W. Jeuken, P. J. Weisbeek, and S. C. M. Smeekens. 1995. Improved performance of transgenic fructan-accumulating tobacco under drought stress. *Plant Physiol.* 107:125–130.

Pontis, H. G. 1989. Fructans and cold stress. *J. Plant Physiol.* 134:148–150.

Rouser, G., S. Fleischer, and A. Yamamoto. 1970. Two dimensional thin layer chromatographic separation of polar lipids and determination of phospholipids by phosphorous analysis of spots. *Lipids.* 5:494–496.

Ryckaert, J. P., G. Giccotti, and H. J. C. Berendsen. 1977. Numerical integration of the Cartesian equation of motion of a system with constraints: molecular dynamics of n-alkanes. *J. Comput. Phys.* 23:327–341.

Seelig, A. 1987. Local anesthetics and pressure, a comparison of dibucarine binding to lipid monolayers and bilayers. *Biochim. Biophys. Acta.* 899:196–204.

Shipley, G. G., J. P. Green, and B. W. Nichols. 1973. The phase behavior of monogalactosyl, digalactosyl, and sulphoquinovosyl diglycerides. *Biochim. Biophys. Acta.* 311:531–544.

Spieser, S. A. H., J. A. van Kuik, L. M. J. Kroon-Batenburg, and J. Kroon. 1999. Improved carbohydrate force field for GROMOS: ring and hydroxymethyl group conformations and exo-anomeric effect. *Carbohydr. Res.* 322:264–273.

Stillwell, W., S. R. Wassall, A. C. Dumaual, W. D. Ehringer, C. W. Browning, and L. J. Jenski. 1993. Use of merocyanine (MC540) in quantifying lipid domains and packing in phopholipid vesicles and tumor cells. *Biochim. Biophys. Acta.* 1146:136–144.

van den Brink-van der Laan, E., R. E. Dalbey, R. A. Demel, J. A. Killian, and B. de Kruijff. 2001. Effect of nonbilayer lipids on membrane binding and insertion of the catalytic domain of leader peptidase. *Biochemistry.* 40:9677–9684.

Vereyken, I. J., V. Chupin, R. A. Demel, S. C. Smeekens, and B. de Kruijff. 2001. Fructans insert between the headgroups of phospholipids. *Biochim. Biophys. Acta.* 1510:307–320.

Vijn, I., and J. C. M. Smeekens. 1999. Fructan: more than a reserve carbohydrate? *Plant Physiol.* 120:351–359.

Wang, N., and P. S. Nobel. 1998. Phloem transport of fructans in the crassulacean acid metabolism species *Agave deserti*. *Plant Physiol.* 116:709–714.

Waterhouse, A. L., T. M. Calub, and A. D. French. 1991. Conformational analysis of 1-kestose by molecular mechanics and n.m.r. spectroscopy. *Carbohydr. Res.* 217:29–42.